



# Diversity in Porous Metal-Organic Framework Materials

Partha Mahata<sup>a</sup> and Srinivasan Natarajan<sup>b</sup>

**Abstract |** The area of metal organic frameworks (MOF) has witnessed rapid growth over the past two decades. The successful synthesis of MOFs depends on the subtle balance between the coordination ability of the metal ion and the organic ligands. The discovery of many new MOF structures over the years suggests that this balance between the organic and the inorganic components have been achieved. The driving force for the study of MOFs, of course, is their potential use in the areas of Lewis acid catalysis, sorption, separation and storage of gases. In this article, we have attempted to highlight the important developments that have taken place during the last decade. In doing so, our focus has been to familiarize the readers with the available diversity in the structures and hence the structural aspects only have been described and discussed.

## 1 Introduction

Porous framework materials have been investigated for their many uses in the areas of gas storage, adsorption based separation, catalysis and drug delivery.<sup>1-3</sup> Traditionally, the porous materials would be either organic or inorganic in nature. The commonly used organic porous material is activated carbon having amorphous porous network structure, and finds many uses that include separation and storage of gases, purification of water, solvent removal and recovery.<sup>4</sup> On the other hand, the inorganic porous materials, the aluminosilicate zeolites, have ordered structures with periodic channels and pores. Syntheses of zeolites require either an inorganic or an organic template, which provide interactions between the inorganic moieties and the template during the synthesis. As a consequence, removal of the template could lead to a collapse of the framework rendering it not useful for the purposes mentioned above. An attractive feature of the zeolite framework is the presence of interconnected channels or cages, which are uniform in size. Uniformity of the pore sizes is attractive for the use as molecular sieve where molecules that are small can fit into the pores while the larger ones are left out. The largest pore diameter in a zeolitic material is limited to about 13 Å. The assembly of surfactants as

micelles has been known, and this behavior was beneficially utilized in the assembly of new forms of silicates—now known as mesoporous silicas. The pore sizes of such compounds can be tuned in the range of 20 to 100 Å. The mesoporous silica materials do not, generally, display uniform pores that are characteristic of natural zeolites. Nevertheless, such inorganic mesoporous frameworks have been employed as catalyst supports as well as in separation applications.<sup>5</sup>

In order to take advantage of the properties of both organic and inorganic porous framework materials, a new generation of compounds known as metal-organic frameworks (MOFs), have been synthesized. These compounds exhibit reasonable thermal stability, high surface area and possess good pores and channel structures.<sup>6</sup> Porous MOFs can be considered as simple coordination compounds with infinite structural possibilities formed by the connectivity between the metal ions/metal clusters and the organic linkers. This opens up the possibility of interplay between the coordination preferences of the metal ions and functionality of the organic ligand leading to fascinating new structural arrangements possessing interconnected channels and pores.<sup>7</sup> One of the important outcomes of the research in the area of MOFs is the control one can have over the pores

<sup>a</sup>Department of Condensed Matter Physics and Material Sciences, S.N. Bose National Centre for Basic Sciences, JD Block, Sector III, Salt Lake City, Kolkata 700 098, India.  
partha.mahata@bose.res.in

<sup>b</sup>Framework Solids Laboratory, Solid State and Structural Chemistry Unit, Indian Institute of Science, Bangalore 560 012, India.  
snatarajan@sscu.iisc.ernet.in

and channels by carefully manipulating the design elements/compatibility between the metal ions and the linkers.<sup>8,9</sup> Some of the MOF structures are also comparable to the well-known zeolites.<sup>10</sup> Many properties such as gas storage, separation, catalysis and related aspects have been explored for this class of compounds.<sup>1-3</sup>

In the present article, a simple overview of some of the recent trends in the design, synthesis and structures of porous MOFs are presented.

## 2 Design Criteria for MOFs

The MOF structure consists of metal ions (connectors) and organic ligands (linkers), which opens up a number of possibilities. One of the important goals in the study of MOFs is to achieve reasonable control over the structures, especially the size and shape of the pores and channels. One can select a number of ligands and match them suitably with the coordination preference of the metal ion to arrive at interesting possibilities in terms of structure. There have been few attempts towards this direction.<sup>11</sup> In this section, we outline some of these design aspects of the MOF structures.

The important characteristics of the connectors and linkers are the coordination numbers, coordination geometries of their binding sites and their charges. Transition-metal ions are often utilized as versatile connectors in the construction of MOFs. Depending on the metal and its oxidation state, coordination numbers can range from 2 to 7, giving rise to various geometries, which can be linear, T- or Y-shaped, tetrahedral, square-planar, square-pyramidal, trigonal-bipyramidal, octahedral, trigonal-prismatic, pentagonal-bipyramidal along with the corresponding distorted forms. The larger coordination numbers of 7 to 10, have coordination geometries like capped octahedral, capped (mono or bi or tri) trigonal-prismatic, dodecahedral, square antiprism etc. The lanthanide ions have been found to be useful for the design of such MOF structures that require larger coordination numbers.

Another way to involve larger coordination numbers is to employ polynuclear clusters constructed from two or more metal ions and organic ligands (generally carboxylate based ligands). They can exhibit larger coordination numbers and newer geometries. This strategy has also been exploited in the design of many MOF structures, wherein the cluster units were employed as connectors.<sup>6</sup>

Important MOF structures have been designed with the classical inorganic structures as the basis. The connectivity between of the connectors and the linkers mimic some of the well known inorganic

structures. The representative networks based on the single coordination geometry for the topologies as well as different coordination numbers are shown in Figure 1. Of the many MOF structures, those based on SrSi<sub>2</sub> (trigonal geometry; Fig. 1a), ThSi<sub>2</sub> (trigonal geometry; Fig. 1b), Diamond (tetrahedral geometry; Fig. 1c), Quartz (tetrahedral geometry; Fig. 1d), NbO (square planar geometry; Fig. 1e), CdSO<sub>4</sub> (square planar geometry; Fig. 1f), α-Po (octahedral geometry; Fig. 1g), CsCl or body centered (cubic geometry; Fig. 1h) and Cu or face centered (icosohedral geometry; Fig. 1i) have been observed repeatedly.

A MOF with a body-centered arrangement has been observed in [Co<sub>2</sub>(μ<sub>3</sub>-OH)(μ<sub>2</sub>-H<sub>2</sub>O)(pyrazine)(OBA)(OBAH)] (OBA = 4,4'-oxybis(benzoate)).<sup>12</sup> In this structure the tetranuclear cobalt cluster [Co<sub>4</sub>(μ<sub>3</sub>-OH)<sub>2</sub>(μ<sub>2</sub>-H<sub>2</sub>O)<sub>2</sub>] units act as the connectors, and the pyrazine and OBA act as linkers to form the CsCl (body centered) network structure (Figure 2).<sup>12</sup> MOF structures have been realized with two different coordination geometries (Figure 3). Thus, MOF structures with boracite (trigonal and tetrahedral; Fig. 3a), Pt<sub>3</sub>O<sub>4</sub> (trigonal and square planar; Fig. 3b), PtS (square planar and tetrahedral; Fig. 3c), rutile (trigonal and octahedral; Fig. 3d), Al<sub>2</sub>O<sub>3</sub> (tetrahedral and octahedral; Fig. 3e) and CaF<sub>2</sub> (tetrahedral and octahedral; Fig. 3f) have been synthesized by careful design.

As an example, the CaF<sub>2</sub> (Fluorite) structure has been observed in [Mn<sub>2</sub>(μ<sub>3</sub>-OH)(H<sub>2</sub>O)<sub>2</sub>(BTC)]·2H<sub>2</sub>O (BTC = 1,2,4-benzenetricarboxylate = trimellitate). In this structure, Mn<sub>4</sub> cluster, [Mn<sub>4</sub>(μ<sub>3</sub>-OH)<sub>2</sub>(H<sub>2</sub>O)<sub>4</sub>O<sub>12</sub>], is connected with eight trimellitate anions, and each trimellitate anion connects to four different Mn<sub>4</sub> clusters, resulting in a fluorite topology (Figure 4).<sup>13</sup> MOF structures have also been designed based on ternary inorganic structures such as perovskite, Na<sub>2</sub>TiS<sub>2</sub> etc. A MOF compound, {[ (CH<sub>3</sub>)<sub>2</sub> NH<sub>2</sub> ] Zn(HCOO)<sub>3</sub> }, with a perovskite related structure has been investigated in recent times. In this compound, (CH<sub>3</sub>)<sub>2</sub> NH<sub>2</sub><sup>+</sup>, Zn<sup>+2</sup> and HCOO<sup>-</sup>, respectively, represent the A, B and X of the perovskite structure, ABX<sub>3</sub> (A-type) (Figure 5).<sup>14</sup>

The Na<sub>2</sub>TiS<sub>2</sub> structure has been realized in [HImd][Mn(BTC)(H<sub>2</sub>O)] (Imd = imidazole; BTC = trimesate).<sup>15</sup> Here the Mn<sub>2</sub> dimer, Mn<sub>2</sub>(COO)<sub>2</sub> unit, is also connected with six trimesate units giving rise to a two dimensional anionic layer of the formula, [Mn(BTC)(H<sub>2</sub>O)]<sup>-</sup> (Figure 6a). The protonated imidazole molecules present in between the two layers act as the charge compensating cation. In this compound, the Mn<sub>2</sub>-dimer is a 6-connected node (connects with six trimesate units) and the trimesate link with three Mn<sub>2</sub>-dimers (3-connected node). The framework can be simplified as a binodal

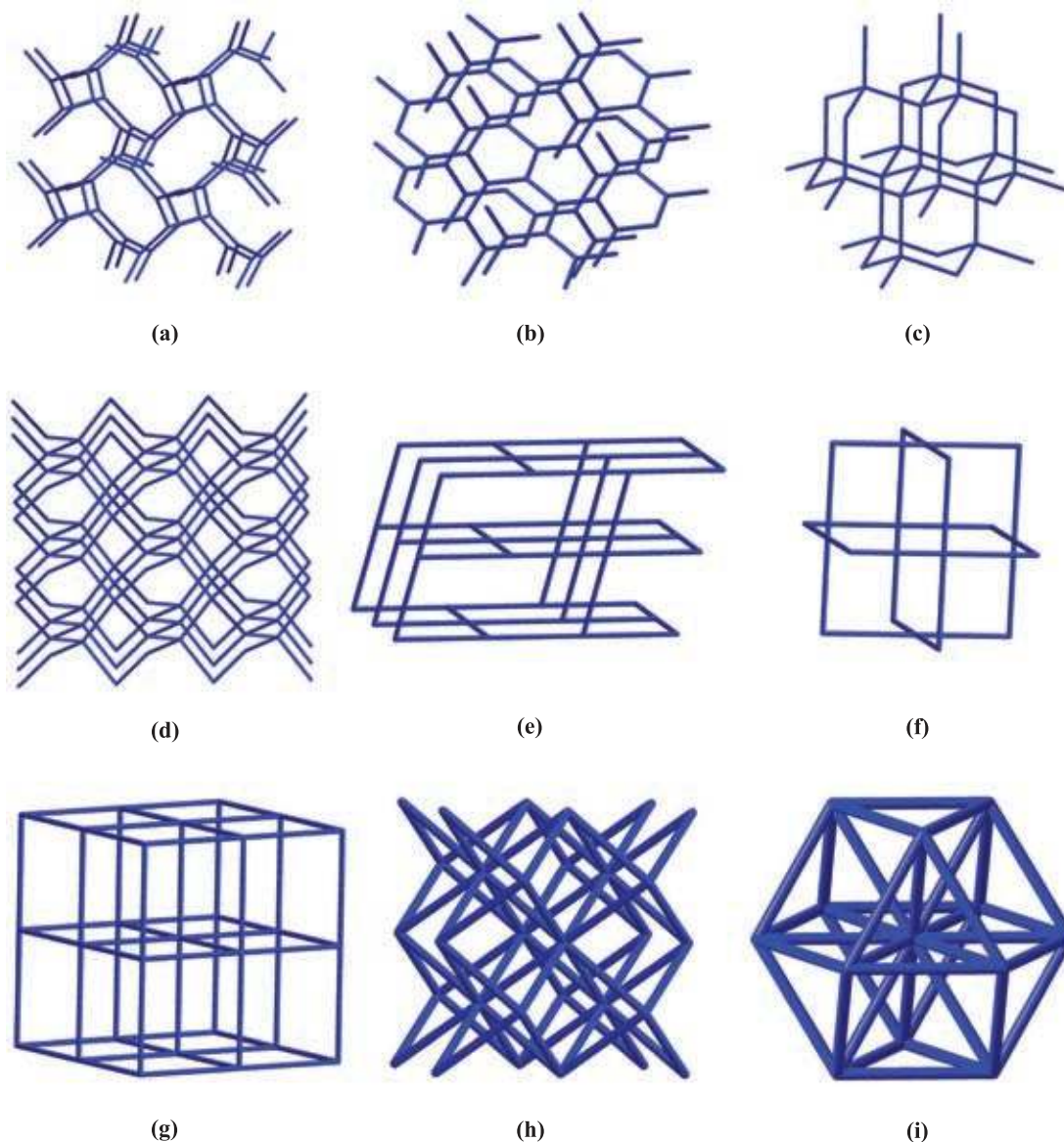


**Figure 1:** Visualization of network topologies based on the single coordination geometry: (a)  $\text{SrSi}_2$ , (b)  $\text{ThSi}_2$ , (c) Diamond, (d) Quartz, (e)  $\text{NbO}$ , (f)  $\text{CdSO}_4$ , (g)  $\alpha\text{-Po}$ , (h)  $\text{CsCl}$  or body centered, (i)  $\text{Cu}$  or face centered.

(6,3)-connected net, which appears to be similar to that observed in  $\text{TiS}_2$  structure (Figure 6b). The protonated imidazole molecules form a honeycomb like two-dimensional arrangement (Figure 6c). This two-dimensional arrangement is similar to the arrangement of the  $\text{Na}^+$  ions within  $\text{TiS}_2$  structure [ $\text{Na}_2\text{TiS}_2$ ] (Figure 6d). It is likely that many other complex structures can be realized by careful choice of the reactants. The research on MOFs is still continuing vigorously in the search for newer and better open structures.

### 3 Synthesis

Experimental conditions play an important role in realizing some of the structures conceptualized

and realized in the previous section. For the synthesis of MOFs, a number of approaches have been attempted, each of which provide a unique solution towards the stabilization of a structure. The chemistry of coordination compounds have been developed over the century, and the MOFs can be considered as an important and interesting twist to this important family. Many of the well established methodology of coordination complexes can be adapted for the synthesis of MOFs. In addition, the open-framework compounds of zeolites and phosphates have been routinely prepared employing hydrothermal methods,<sup>16</sup> which was also used for the synthesis of MOFs. In the hydro/solvothermal method,

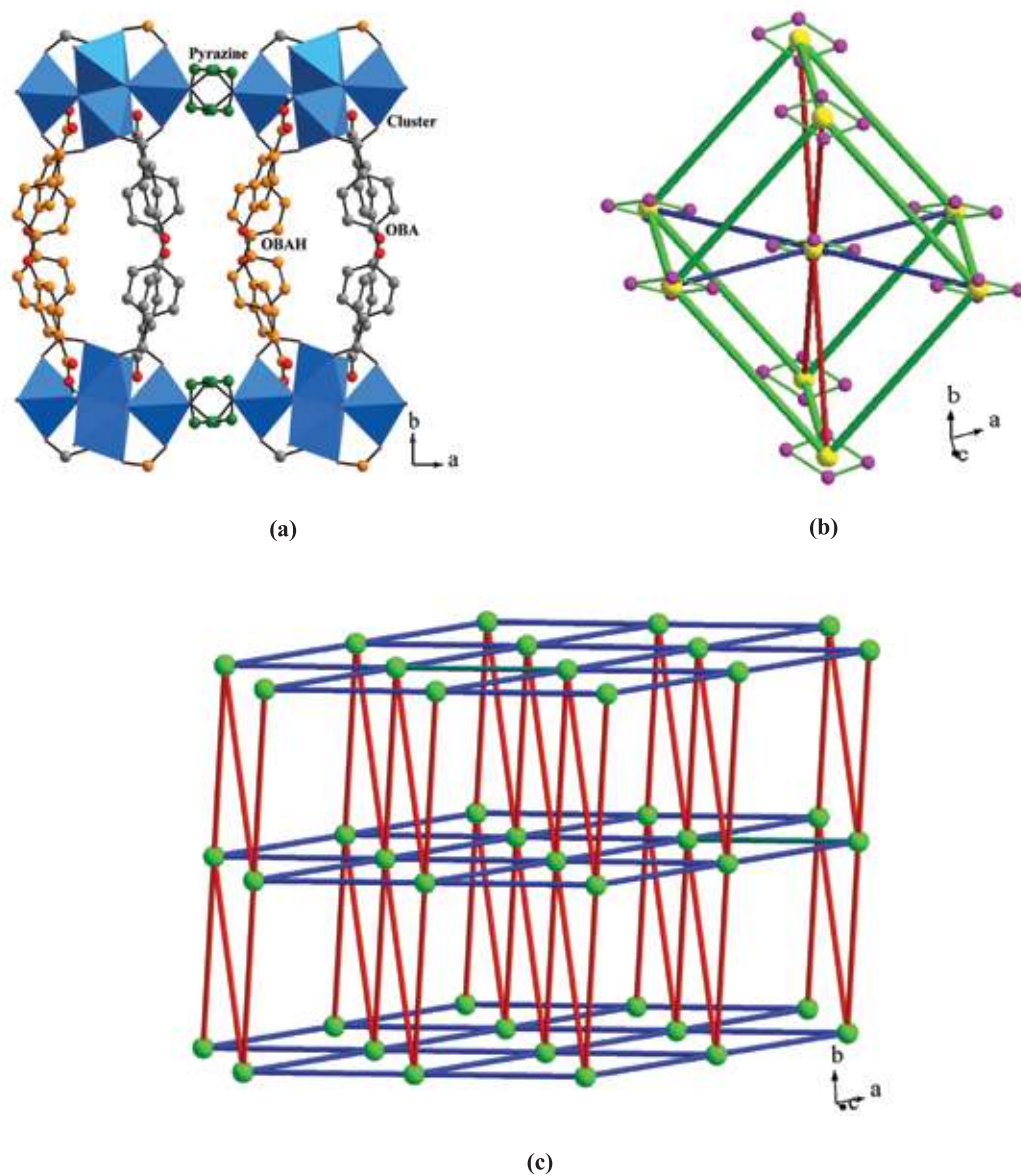


**Figure 2:** (a) View of the three-dimensional connectivity in  $[\text{Co}_2(\mu_3\text{-OH})(\mu_2\text{-H}_2\text{O})(\text{pyrazine})(\text{OBA})(\text{OBAH})]$ . (b) Figure shows the Body Centered like unit based on the tetranuclear cluster connected through pyrazine (blue line) and OBA (red line) unit. (Yellow sphere—centroid of the  $\text{Co}_4$  cluster, green line—cell edge of the elementary BC cell). (c) Three-dimensional connectivity of the cluster (green sphere) with pyrazine (blue line) and OBA unit (red line) to form CsCl network (Ref. 12).

the reactants are heated in a closed reaction vessel at temperatures in the range of 100–250 °C. Recent studies suggested that for a particular composition, the temperature effects are profound leading to the formation of more dense framework through an entropy driven dehydration pathway.<sup>17–19</sup>

The use of liquid-liquid interphase is another elegant approach that has been used extensively for the synthesis of MOFs.<sup>20</sup> In this method, the metal ions are taken in a particular solvent (usually polar) and the organic ligand in another solvent (Figure 7). This method generally employs room

temperature, though high temperatures have also been used. The surface tension at the inter-phase boundary between the two liquids is employed beneficially to prepare new MOFs. This approach depends on the migration of species across the inter-phase boundary, employs milder reaction conditions, and generally result in open structures.

In addition to these common methods, many newer techniques such as electrochemical, microwave assisted and mechanochemical approaches have been employed with good results. A variant of some of these techniques outlined here is the high



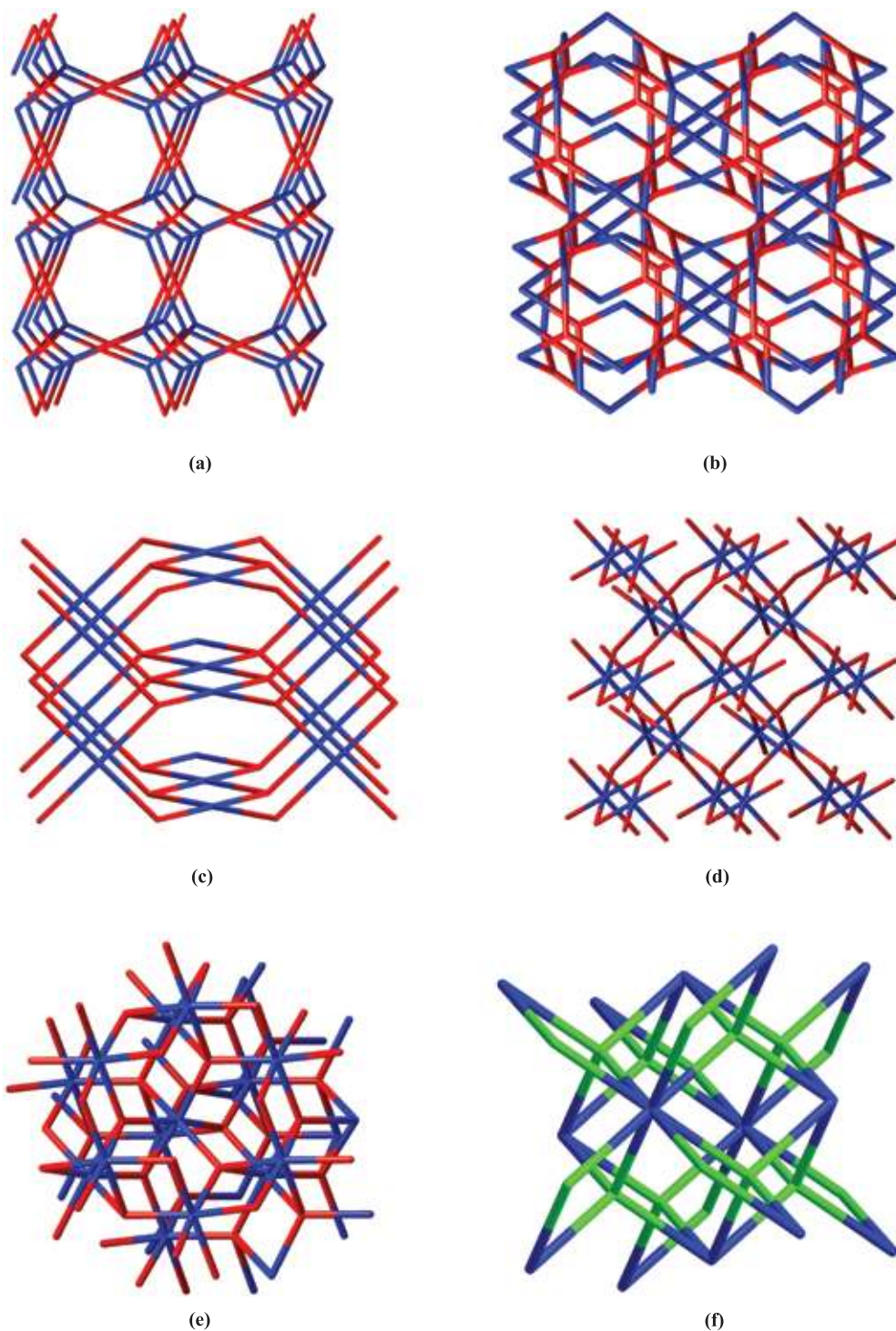


**Figure 3:** Visualization of network topologies based on two different coordination geometries: (a) boracite, (b) Pt<sub>3</sub>O<sub>4</sub>, (c) PtS, (d) rutile, (e) Al<sub>2</sub>O<sub>3</sub>, (f) CaF<sub>2</sub>.

throughput method; this method is well established in organic synthesis and the approach has been elegantly adapted for the preparation of MOFs. Accordingly, a number of compositions and variations can be examined simultaneously resulting in interesting new findings.<sup>21</sup>

#### 4 Important Structures

Research on metal-organic framework compounds is maturing with the discovery of many interesting structures. Of the many structures, the earliest and notable ones belong to MOF-5[Zn<sub>4</sub>O(1,4-benzene diacrylate)<sub>3</sub>(DMF)<sub>8</sub>(C<sub>6</sub>H<sub>5</sub>Cl)]<sup>22</sup> and HKUST-1

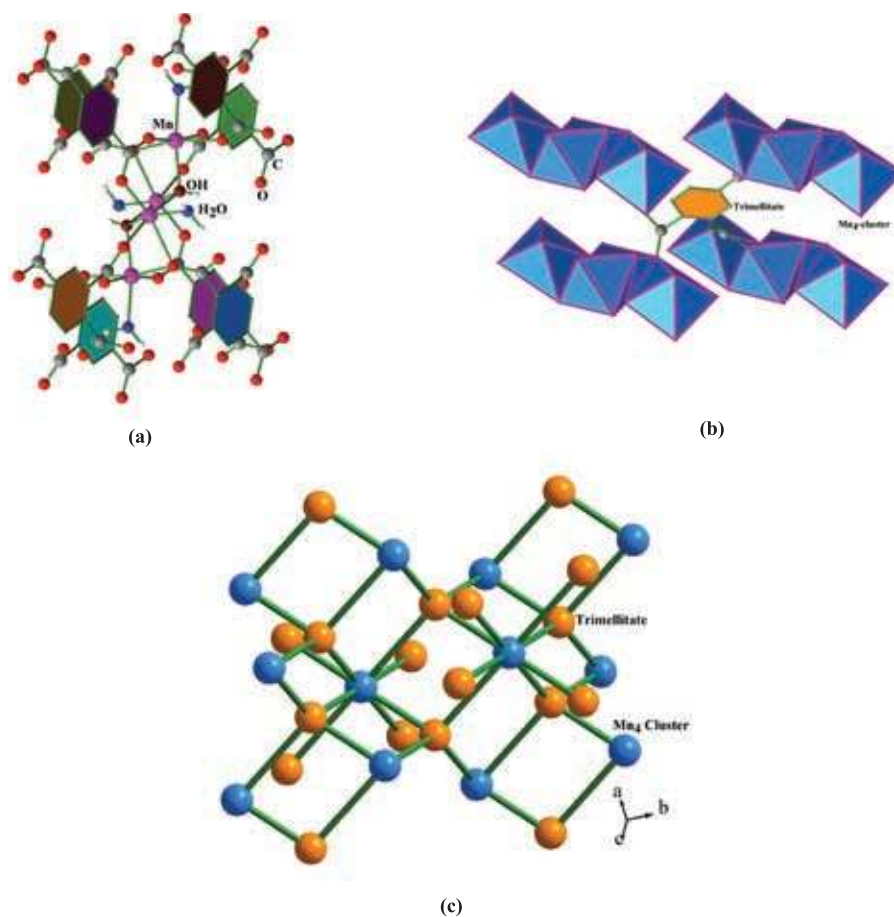


**Figure 4:** (a) Figure shows that each Mn<sub>4</sub> cluster is connected eight different trimellitate anions in Mn<sub>2</sub>(μ<sub>3</sub>-OH)(H<sub>2</sub>O)<sub>2</sub>(BTC)]·2H<sub>2</sub>O. (b) Figure shows that each trimellitate anion is connected with four different Mn<sub>4</sub> clusters. (c) Structure showing the connectivity between the 8-connected Mn<sub>4</sub> clusters and the 4-connected trimellitate anions. Note the close resemblance with the CaF<sub>2</sub> structure (Fig. 3f) (Ref. 13).

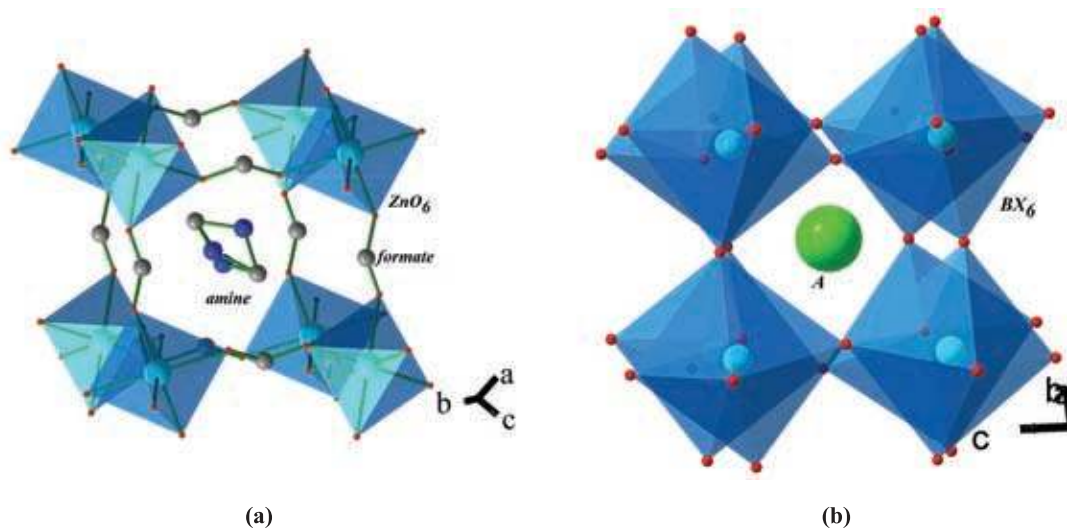


**Figure 5:** (a) Figure shows the connectivity between Zn<sup>2+</sup> ions and HCOO<sup>-</sup> anions (formate) with [(CH<sub>3</sub>)<sub>2</sub>NH<sub>2</sub>]<sup>+</sup> ion at the middle forming perovskite structure in [(CH<sub>3</sub>)<sub>2</sub>NH<sub>2</sub>]Zn(HCOO)<sub>3</sub>. (b) The ideal perovskite structure with the general formula of ABX<sub>3</sub>. Note the similarity between the two structures (Ref. 14).

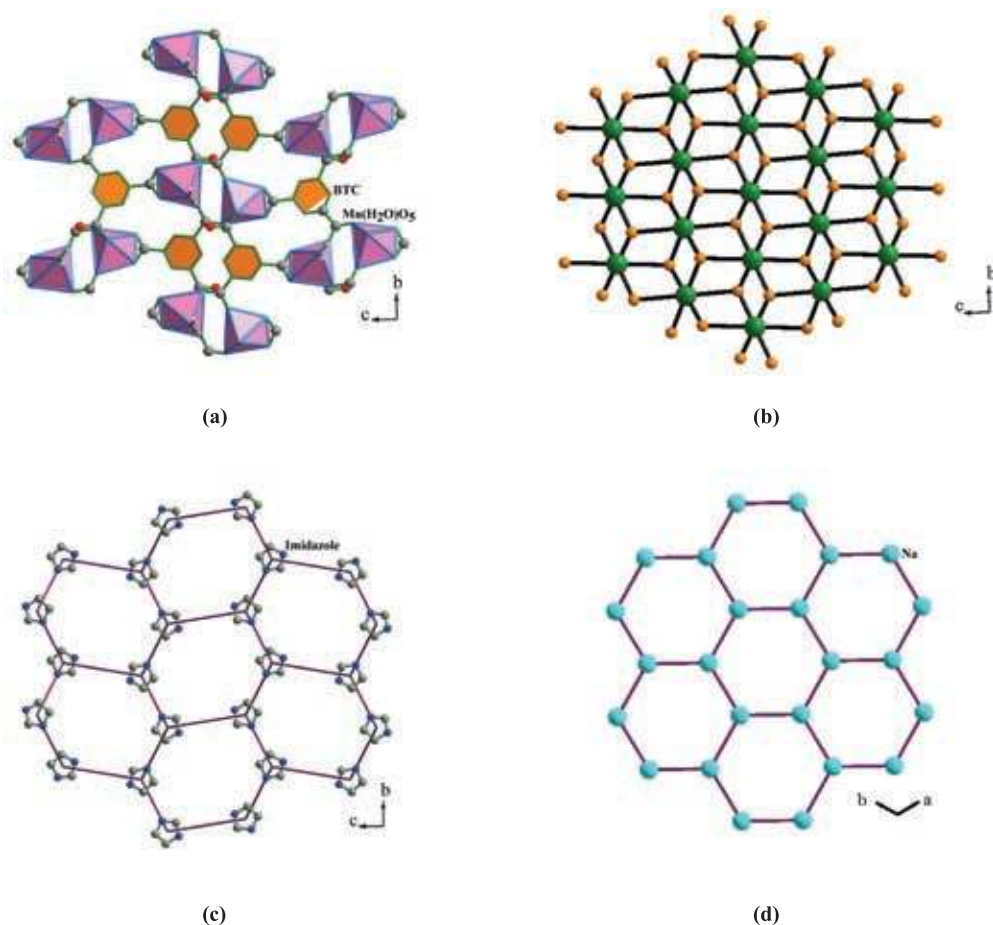


**Figure 6:** (a) Figure shows that each  $Mn_2$  dimer is connected six different trimesate anions and each trimesate anion is connected with three different  $Mn_2$  dimers in  $[Hlmd][Mn(BTC)(H_2O)]$  (lmd = imidazole; BTC = trimesate). (b) Schematic representation of the connectivity between the six connected  $Mn_2$  dimeric units (green) and the three connected trimesate anions (orange), which is similar with the structure of  $TiS_2$ . (c) Figure shows the arrangement of the imidazole molecules in the inter-layer space of  $[Hlmd][Mn(BTC)(H_2O)]$ . Note the formation of  $6^3$  net (honeycomb). (d) Figure shows the arrangement of  $Na^+$  in the inter-layer space of  $TiS_2$ . Note the close similarity between the arrangement of protonated imidazole and  $Na^+$  ions (Ref. 15).

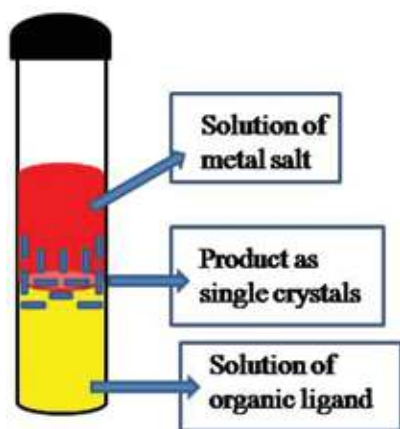


**Figure 7:** Schematic representation of biphasic reactions procedure for the synthesis of MOFs.

$[Cu_3(1,3,5\text{-benzenetricarboxylate})_2(H_2O)_3]$ .<sup>23</sup> Extensive studies over the years have rendered these compounds to be prepared in a variety of ways that include thin-films,<sup>24</sup> membranes<sup>25-26</sup> etc. In addition to these, compounds generally known as MIL (Material Institut Lavoisier) have also attracted attention.<sup>5</sup> Structural aspects of MOF-5 and HKUST have been described and discussed in many reviews and monographs. Here, we present the MIL structure, MIL-53  $[M(1,4\text{-bdc})(\mu_3\text{-OH})]$  ( $M = Al, Cr, Fe$ ).<sup>27-30</sup> The other notable structure is the MIL-101  $[Cr_3(O)(1,4\text{-bdc})_3(F)(H_2O)_2] \cdot \sim 25H_2O$ , the structure of which was established by a clever combination of synthesis, high resolution powder x-ray diffraction studies and computational approaches.<sup>31</sup> These compounds have attracted the attention of many synthetic chemists due to their extraordinary robustness and thermal stability, which are



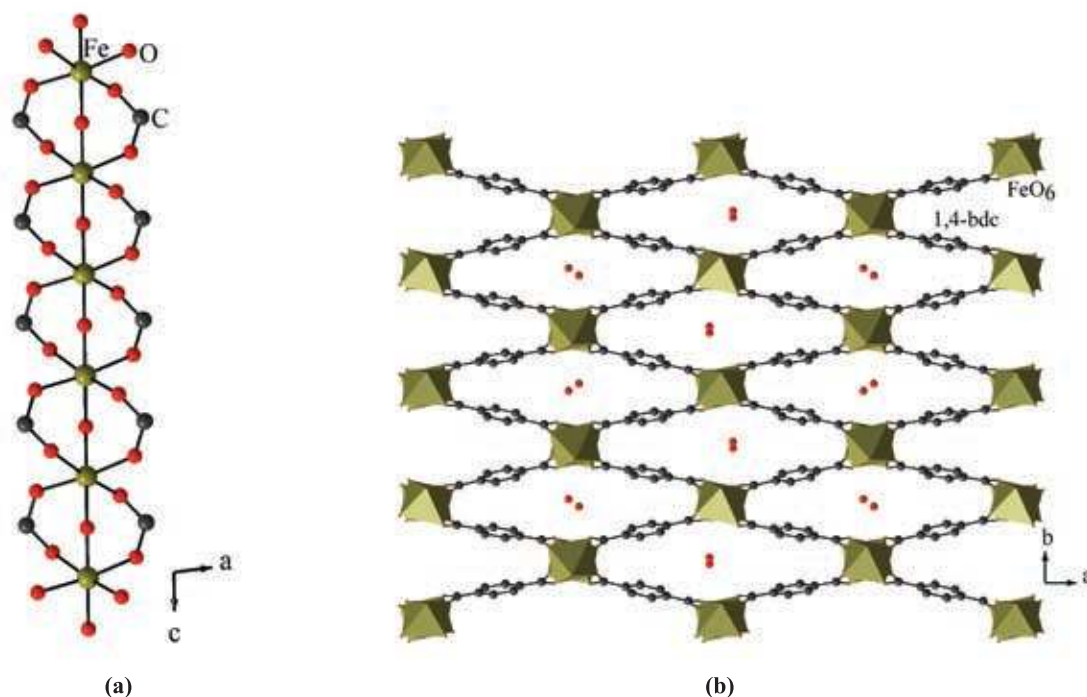


**Figure 8:** (a) Figure shows the structure of one dimensional infinite -Fe-O-Fe- chains in MIL-53 [Fe(1,4-bdc)( $\mu_3$ -OH)]·H<sub>2</sub>O. (b) View of the three-dimensional structure of MIL-53(Fe) based on the connectivity of one dimensional infinite -Fe-O-Fe- chains and 1,4-benzenedicarboxylates. Note the formation of water filled one-dimensional channels running parallel to the c-axis (Ref. 29).

important for post-synthetic modifications and use in areas such as catalysis, sorption and separation.

The three dimensional structure of MIL-53 (Fe)<sup>29</sup> can be described based on the connectivity of the one dimensional infinite -Fe-O-Fe- chains and the 1,4-benzenedicarboxylate anions (Figure 8a). This structure is built up from corner-sharing trans chains of Fe octahedral linked by 1,4-benzenedicarboxylate moieties to form an open framework with one-dimensional channels running parallel to the c-axis (Figure 8b). Water molecules are located at the centre of the channels. The synthesis of Fe- based MOF was an important step as they opened up studies in the areas of magnetic, catalytic and biological applications.

The use of nitrogen containing ligands in the assembly of MOF structures have resulted in a number of important structures. The structures based on imidazole would be discussed separately. The other nitrogen containing ligands such as 2,4, 6-tris(4-pyridyl)-1,3,5-triazine (TPT) and related ones have been employed gainfully. Fujita and coworkers exploited the nitrogen containing aromatic ring to prepare a number of important MOF structures. Of these, mention must be made on the synthesis of [(ZnI<sub>2</sub>)<sub>3</sub>(TPT)<sub>2</sub>(triphenylene)(Solvent)<sub>x</sub>], a bi-porous MOF (Figure 9).<sup>32</sup> This compound has been used as molecular flask to

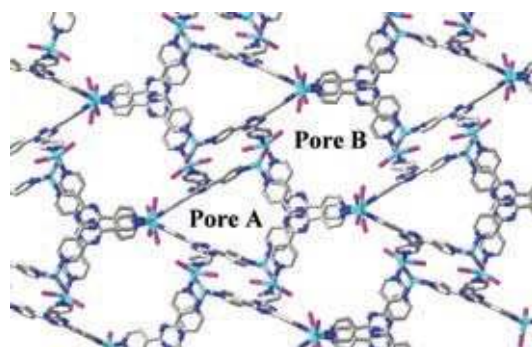


**Figure 9:** Structure of [(ZnI<sub>2</sub>)<sub>3</sub>(TPT)<sub>2</sub>(triphenylene)(Solvent)<sub>x</sub>] (TPT = tris(4-pyridyl) triazine). The guest triphenylene and solvent molecules are not shown for clarity. The figure shows two different kinds of pores (Ref. 32).

carry out many organic reactions, which stabilized unusual intermediates and products.<sup>33</sup> Recently, this compound was also used to determine the structures of many natural products. The approach was to absorb nanogram to microgram quantity of the natural product within the pore of the MOF and subject the MOF to single crystal x-ray diffraction studies.<sup>34</sup> This approach offers a new methodology in determining the conformation as well as the structures of natural products, which are otherwise determined employing



a combination methods such as NMR, chemical analysis, MALDI-TOF etc.

## 5 Imidazole Based Structures

The metal-organic frameworks with topological features characteristic of 4-connected zeolites have been attempted. Among various efforts to extend zeolitic frameworks in MOFs use of tetrahedral imidazolate frameworks has been particularly successful in tuning both compositional and topological features. In 4-connected imidazolate frameworks, divalent metal ions (such as  $\text{Zn}^{2+}$ ,  $\text{Co}^{2+}$  etc.) replace the traditional tetrahedral T atoms (Si). Imidazolate ( $\text{im}^-$ ) ions substitute for the bridging  $\text{O}^{2-}$  in the zeolite structures, which result in a number of 4-connected frameworks. Similar to the pure siliceous zeolites, all of which have the formula  $\text{SiO}_2$ , the imidazolate frameworks also have the general framework composition of  $\text{M}(\text{im})_2$ . The formation of zeolitic topologies using the imidazolate ligands can be understood by comparing the bonding patterns between zeolites and zeolitic imidazolate frameworks (ZIFs). In ZIFs, the two coordinate N atoms are oriented in such way that the M-Im-M angle is about  $144^\circ$ , which is comparable to the mean Si-O-Si angle of  $145^\circ$  in many zeolites.

The first study of the zeolite-like structure in MOFs is  $[\text{Co}(\text{im})_2] \cdot 0.4 \text{ MB}$  (MB = 3-methyl-1-butanol).<sup>35</sup> The robustness of the porous and open framework was established by exchanging the included template with EtOH. EtOH can be removed under vacuum, which renders a porous compound.  $[\text{Co}(\text{im})_2]$  was extended to other isomeric zeolite-like and zeolitic (*neb*, *zni*, *cag*, *BCT*) frameworks by use of different template and/or structure directing agent under solvothermal conditions. The compounds were found to be nonporous or collapse after the removal of the guest molecule. Some of them exhibit interesting magnetic properties due to the canting of the magnetic spins.<sup>36,37</sup>

A series of zinc imidazolates with symmetrical porous structures analogous to the zeolites have been prepared and their structures determined.<sup>38</sup> Using the imidazolate ligands with different substituent at the 2-position, three compounds,  $[\text{Zn}(\text{mim})_2] \cdot 2\text{H}_2\text{O}$ ,  $[\text{Zn}(\text{eim})_2] \cdot \text{H}_2\text{O}$  and  $[\text{Zn}(\text{eim/mim})_2] \cdot 1.25\text{H}_2\text{O}$  (Hmim = 2-methylimidazole, Heim = 2-ethylimidazole) have been isolated. In all the compounds,  $\text{Zn}^{2+}$  ion are tetrahedrally coordinated by four nitrogen atoms of four imidazolates ligands and each of imidazolates connects with two  $\text{Zn}^{2+}$  ions (Figure 10a and 10b). Topological analysis of  $[\text{Zn}(\text{mim})_2] \cdot 2\text{H}_2\text{O}$  using the  $\text{Zn}^{2+}$  ion as 4-connected node shows zeolitic sodalite (SOD) topology (Figure 10c). It has a solvent-accessible volume of

47% of the available crystal volume. This value is comparable to the void fractions of 0.47–0.50 for the open zeolites such as the faujasite, paulingite, and zeolite A.  $[\text{Zn}(\text{eim})_2] \cdot \text{H}_2\text{O}$  has the analcime (ANA) topology with 38.6% solvent solvent-accessible volume. Formation of two different topologies employing simple substituents in the 2-position of imidazole suggests the versatility of these compounds. Using a mixture of 2-methylimidazole and 2-ethylimidazole,  $[\text{Zn}(\text{eim/mim})_2] \cdot 1.25\text{H}_2\text{O}$  has been isolated, which has rho (RHO) topology with 55.4% solvent-accessible volume that is larger than the other two compounds.

A series of ZIF structures (known as ZIF-1 to ZIF-12) employing  $\text{Zn}^{2+}$ ,  $\text{Co}^{2+}$  and mixture of  $\text{In}^{3+}$  and  $\text{Zn}^{2+}$  ions have been prepared.<sup>39</sup> Six different compounds with four different zeolitic topologies having the same framework formula,  $[\text{Zn}(\text{im})_2]$  have been prepared by modifying the synthesis conditions. The observed zeolitic topologies are:  $[\text{Zn}(\text{im})_2]$  are *BCT* (ZIF-1, ZIF-2), *DFT* (ZIF-3), *GIS* (ZIF-6) and *MER* (ZIF-10), and ZIF-4 has the  $\text{CaGa}_2\text{O}_4$  (*cag*) topology. *SOD* and *RHO* topologies have also been observed employing benzimidazole and 2-methylimidazole.<sup>38</sup> The use of mixed metals with different coordination preferences result in  $[\text{In}_2\text{Zn}_3(\text{im})_{12}]$  with  $\text{In}^{3+}$  in octahedral and  $\text{Zn}^{2+}$  in tetrahedral coordination environment. This structure has the same formula and topology as the garnet,  $\text{Ca}_3\text{Al}_2\text{Si}_3\text{O}_{12}$ . It may be noted that the variations in the angles of the  $-\text{M}-\text{Im}-\text{M}-$  could have contributed to the observation of close but dissimilar topologies in some of the structures described herein. This observation is similar to the idea that the differences in the Si-O-Si angle is the reason for the observation of different zeolitic structures, though all zeolites have the same building unit,  $\text{SiO}_4$ .

The research in this area depends on the organic chemistry, especially the design and synthesis of newer organic ligands, which can be fine tuned to prepare both known and unknown topologies. Thus, benzimidazole has been modified to form new structures.<sup>40</sup> Thus, Zeolite A (LTA) topology with two types of cages ( $\alpha$  and  $\beta$ ) has been prepared. When the carbon atom in the 4-position of benzimidazolate is replaced by N atom (4-Azabenzimidazolate), it forms a ZIF structure  $[\text{Zn}(4\text{-Azabenzimidazolato})_2] \cdot 0.25\text{H}_2\text{O}$  (ZIF-23) with diamond topology. Replacing the carbon atoms at other positions, however, leads to ZIFs with LTA topology:  $[\text{Zn}(\text{pur})_2] \cdot 0.75\text{DMF} \cdot 1.5\text{H}_2\text{O}$  (pur = purinate; ZIF-20),  $[\text{Co}(\text{pur})_2] \cdot \text{DMF} \cdot \text{H}_2\text{O}$  (ZIF-21) and  $[\text{Zn}(5\text{-Azabenzimidazolato})_2] \cdot 0.75\text{DMF} \cdot 2\text{H}_2\text{O}$  (ZIF-22). The findings suggest of the interactions between the linkers having a profound effect on the topology of the structures.

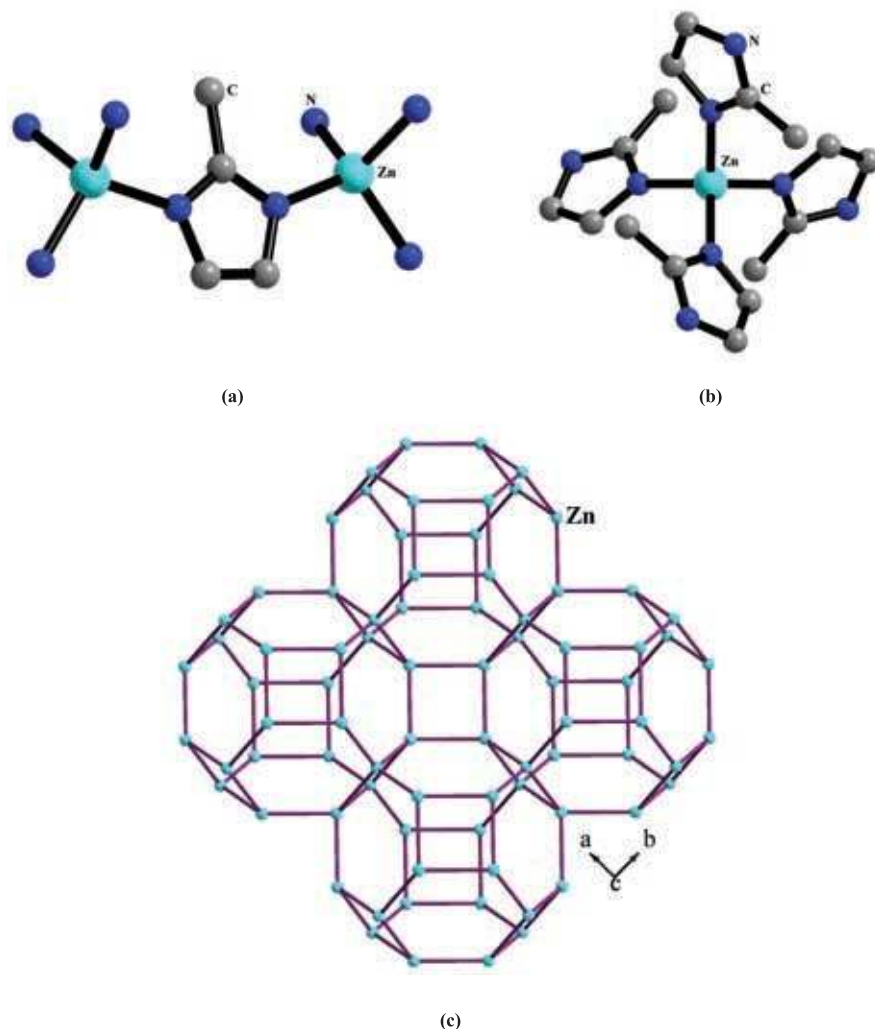


**Figure 10:** (a) Figure shows the connectivity between 2-methylimidazolate and  $Zn^{+2}$  ions in  $[Zn(mim)_2]$  (mim = 2-methylimidazolate; ZIF-8). (b) Figure shows the connectivity of the  $Zn^{2+}$  ions. Note that four 2-methylimidazolate units connect with one  $Zn^{2+}$  ion. (c) Figure shows the connectivity between  $Zn^{2+}$  ions through 2-methylimidazolate units forming the sodalite network (Ref. 38).

The discovery of a large family of MOFs with zeolitic frameworks has attracted considerable number of researchers towards this area resulting in many zeolitic and related structures based on different types of imidazoles.<sup>41–43</sup> The important ZIF structures are given in Table 1.

## 6 Uses of Amino Acids in the Formation of Porous MOFs

The use of amino acids as a network builder promises further diversity, both in the functionality and applicability of MOFs. In addition, the different sidearm residues of the amino acids add further intrigue towards the chelating ability of the amino acids. In spite of the considerable interest, the number of three-dimensional MOFs with amino acid backbones are not

many.<sup>44–49</sup> Three-dimensional MOF,  $[Ni_2(L-asp)_2(bipy)] \cdot 1.28CH_3OH \cdot 0.72H_2O$  (L-asp = L-Aspartate, bipy = 4,4'-bipyridine), using pure amino acid and 4,4'-bipyridine was reported recently.<sup>44</sup> The compound has chiral Ni(L-asp) layers cross-linked by bipyridine to form the three-dimensional structure. The nickel centers are connected differently by the aspartate molecules forming the layer (Figure 11a). The layers are connected by the 4,4'-bipyridine to form three-dimensional structures (Figure 11b). The distance between the 4,4'-bipyridine pillars connecting two Ni(L-asp) layers is 7.73 Å, and the interlayer distance between the nickel cations linked by the 4,4'-bipyridine molecules is 9.5 Å. The resulting channels which run along the b direction have a narrowest cross section of 3.8 X 4.7 Å (including van der Waals radii), and

**Table 1:** Summary of the important ZIF structures.

Formula of the frameworks	Name of ligands	Topologies	References
[Co(im) <sub>2</sub> ]	Imidazole	nog	35
[Zn(im) <sub>2</sub> ]	Imidazole	coi	36
[Cd(im) <sub>2</sub> ]	Imidazole	Dia	36
[Co(im) <sub>2</sub> ]	Imidazole	neb	36
[Co(im) <sub>2</sub> ]	Imidazole	zni	36
[Co(im) <sub>2</sub> ]	Imidazole	cag	37
[Co(im) <sub>2</sub> ]	Imidazole	BCT	37
Zn(mim) <sub>2</sub>	2-methylimidazole	SOD	38, 39
Zn(eim) <sub>2</sub>	2-ethylimidazole	ANA	38
Zn(eim/mim) <sub>2</sub>	2-methylimidazole/2-ethylimidazole	RHO	38
Zn(im) <sub>2</sub>	Imidazole	BCT	39
Zn(im) <sub>2</sub>	Imidazole	DFT	39
Zn(im) <sub>2</sub>	Imidazole	GIS	39
Zn(im) <sub>2</sub>	Imidazole	MER	39
Zn(im) <sub>2</sub>	Imidazole	cag	39
Zn(bim) <sub>2</sub>	Benzimidazole	SOD	39
Co(bim) <sub>2</sub>	Benzimidazole	RHO	39
In <sub>2</sub> Zn <sub>3</sub> (im) <sub>12</sub>	Imidazole	Ca <sub>3</sub> Al <sub>2</sub> Si <sub>3</sub> O <sub>12</sub>	39
Zn(4-Azabenzimidazolato) <sub>2</sub>	4-Azabenzimidazolate	Dia	40
Zn(pur) <sub>2</sub>	purinate	LTA	40
Co(pur) <sub>2</sub>	purinate	LTA	40
Zn(5-Azabenzimidazolato) <sub>2</sub>	5-Azabenzimidazolate	LTA	40
Zn(im) <sub>1.5</sub> (mim) <sub>0.5</sub>	Imidazole, 2-methylimidazole	MER	41
Co(nim) <sub>2</sub>	nitroimidazole (Hnim)	SOD	41
Co(mim) <sub>2</sub>	2-methylimidazole	SOD	41
Zn(bim)(nim)	Benzimidazole, 2-nitroimidazole (Hnim)	GME	41
Zn(cbim)(nim)	5-chlorobenzimidazole, 2-nitroimidazole (Hnim)	GME	41
Zn(im) <sub>1.13</sub> (nim) <sub>0.87</sub>	Imidazole, 2-nitroimidazole (Hnim)	GME	41
Zn(nim)(dbim)	2-nitroimidazole (Hnim), 5,6-dimethylbenzimidazole	GIS	41
Co(nim)(dbim)	2-nitroimidazole (Hnim), 5,6-dimethylbenzimidazole	GIS	41
Zn(im) <sub>2</sub>	Imidazole	BCT	41
Zn(dcim) <sub>2</sub>	4,5-dichloroimidazole	RHO	41
Zn(im)(cbim)	Imidazole, 5-chlorobenzimidazole	LTA	41



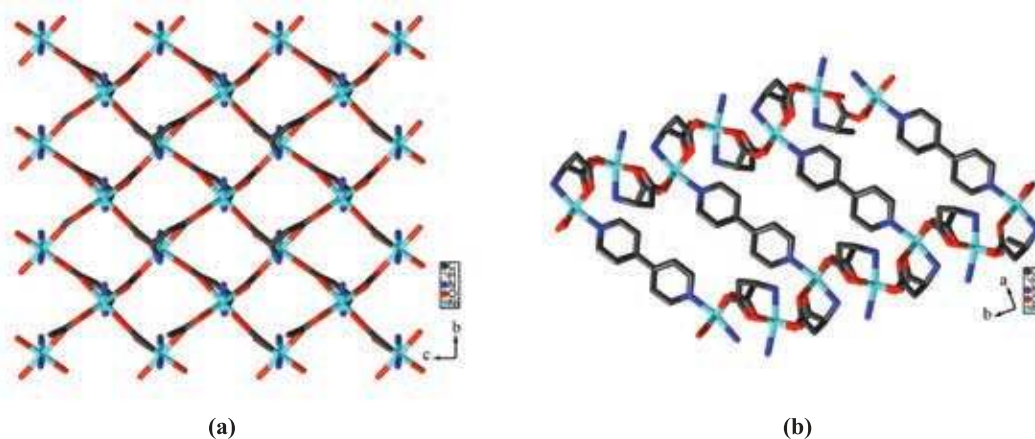


**Figure 11:** (a) Figure shows the connectivity between  $\text{Ni}^{2+}$  ions and aspartate molecules forming layer structure in  $[\text{Ni}_2(\text{L-asp})_2(\text{bipy})] \cdot 1.28\text{CH}_3\text{OH} \cdot 0.72\text{H}_2\text{O}$  (L-asp = L-Aspartate, bipy = 4,4'-bipyridine). (b) View of connectivity between layers through the 4,4'-bipyridine to form three-dimensional structures (Ref. 44).

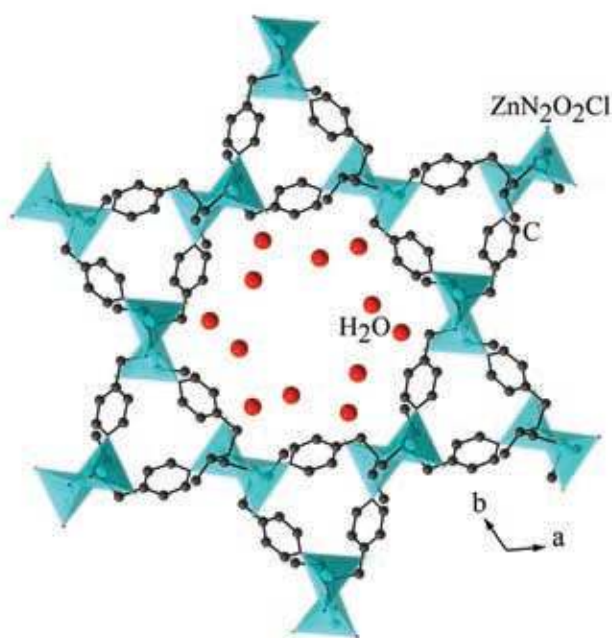


**Figure 12:** Polyhedral representation of the structure of  $[\text{AlaZnCl}]$  (Ala = deprotonated 2-(pyridine-4-yl-methylamino)propanoic acid) viewed down the c-axis. Cyan polyhedra represent zinc centers, and lattice water molecules are shown as red balls (Ref. 46).

account for a solvent-accessible volume of 23.1% of the total volume of the MOF. The projection of the chiral carbon atoms of the aspartate units into the channels imparts chirality to the internal surface of the material.

Banerjee and co-workers extended the use of amino acid derived linkers (pyridyl functionalized) to form a number of MOF compounds.<sup>45–49</sup> Careful design of the linker molecules employing alanine, valine, threonine, leucine and serine led to newer MOFs including one with a

zeolitic *unh* topology. The compound,  $[\text{AlaZnCl}]$  (Ala = deprotonated 2-(pyridine-4-yl-methylamino)propanoic acid),<sup>46</sup> crystallized in chiral  $P6_1$  space group, has  $\text{Zn}^{2+}$  ions in distorted square pyramidal geometry with Cl atom occupying the axial position. Each  $\text{Zn}^{2+}$  ion is connected with four other  $\text{Zn}^{2+}$  ions through the alanine moiety forming the *unh* topology (Figure 12). There have been attempts at preparing newer MOFs employing aromatic amine substituted carboxylic acids.<sup>50</sup>

## 7 Sugars as Building Units in MOFs

Majority of the MOFs described are generally based on organic linkers derived from non-renewable petrochemical feedstocks and transition/main group metals. The challenge in preparing MOFs from natural products lies in the inherent asymmetry of the building units, which are not amenable to crystallization in the form of highly porous frameworks. The synthesis of MOF compounds from edible natural products was reported recently.<sup>51,52</sup> The use of  $\gamma$ -cyclodextrin ( $\gamma$ -CD) (Fig. 13a), a symmetrical cyclic oligosaccharide

that is mass-produced enzymatically from starch and comprises eight asymmetric  $\alpha$ -1,4-linked D-glucopyranosyl residues and potassium ions, forms the MOF,  $[(C_{48}H_{80}O_{40})(KOH)_2]$ .<sup>51</sup> This MOF has been prepared entirely from edible ingredients – food-grade  $\gamma$ -CD, KCl or potassium benzoate (food additive E212) in bottled water and everclear grain spirit (EtOH). Isostructural MOFs using  $Na^+$ ,  $Rb^+$ , and  $Cs^+$  ions in place of  $K^+$  ions have also been prepared and characterized. The X-ray crystal structure of  $[(C_{48}H_{80}O_{40})(KOH)_2]$  reveals that eight-coordinate  $K^+$  ions not

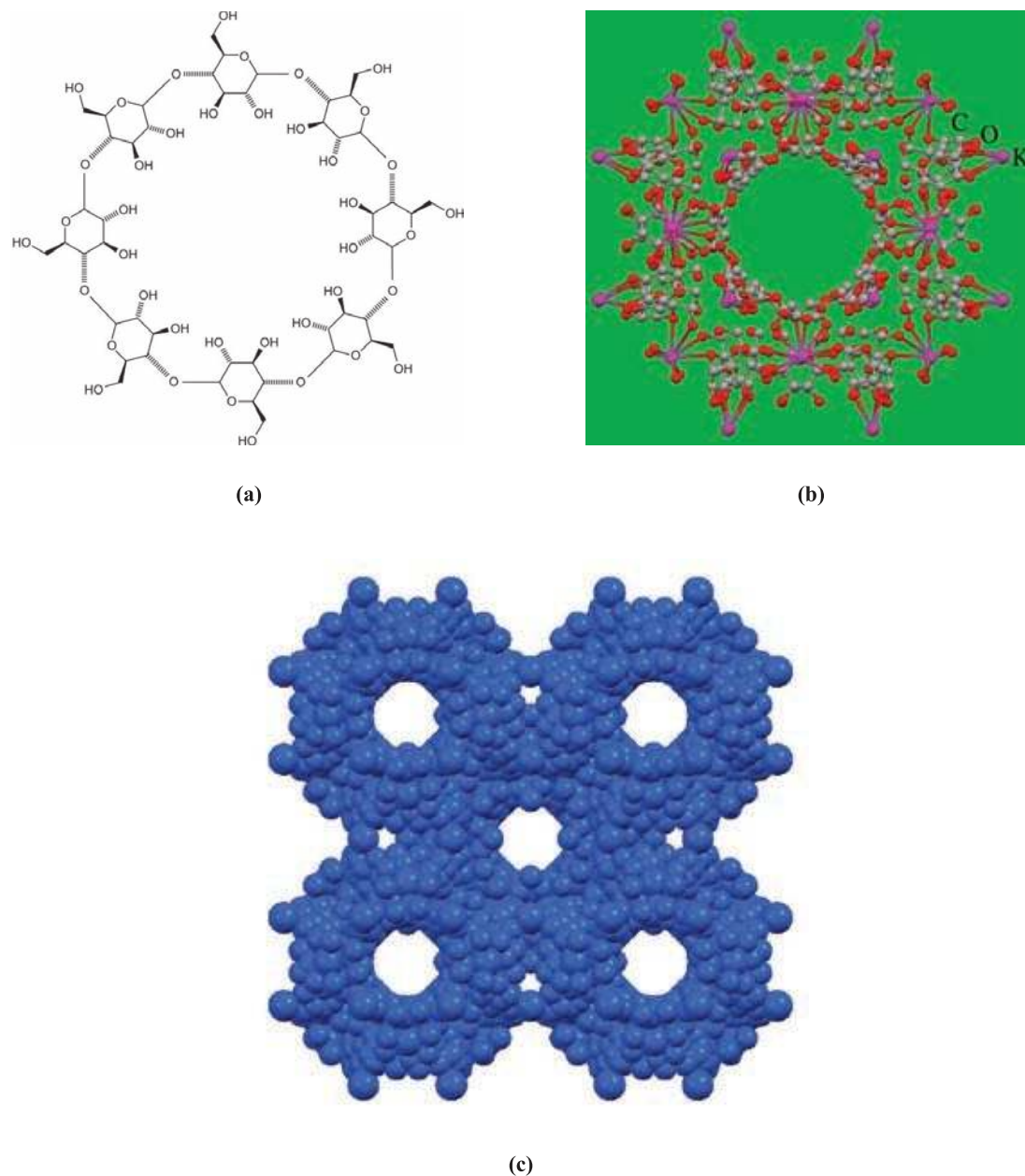


**Figure 13:** (a) Schematic structure  $\gamma$ -cyclodextrin ( $\gamma$ -CD). (b) A ball-and-stick representation of the structure of  $[(C_{48}H_{80}O_{40})(KOH)_2]$ . (c) A space-filling representation of the extended solid-state structure, showing the  $(\gamma\text{-CD})_6$  repeating motifs adopting a body-centered cubic packing arrangement (Ref. 51).

only assist in the assembly of  $(\gamma\text{-CD})_6$  cubes (Figure 13 b), wherein six  $\gamma\text{-CD}$  units occupy the faces of a cube, but also serve to link the cubes into a three-dimensional array (Figure 13c). The framework has an estimated total pore volume of 54%.

## 8 Conclusions

The area of metal-organic frameworks has witnessed considerable growth during the last two decades, which in many ways is similar to that observed during the high temperature superconductivity research of late 80's and early 90's. This suggests that these are important compounds with very high potential. From the above descriptions, it becomes clear that the structural diversity of MOFs is very high. More importantly, the ability to tune and design the structure using some of the well established principles of crystal engineering of organic chemistry coupled with inorganic coordination chemistry provides a fine handle for the synthetic chemist to exploit. It must be noted the design of the organic linkers is still the focus for obtaining the control on the structure and functionality of porous MOF structures.

Importance of molecular coordination compounds for several applications has been established over many decades. The combined design by transposing the complexes within the MOFs by employing the building blocks approach is an emergent and important area of research to develop functional MOF architectures. The various examples in the literature indicate that this strategy allows better control of the properties of the final network, since the building blocks (i.e., molecular complexes) are rigid, chemically stable and maintain their activity within the MOF structure.

One of the possible impediments in the growth, if one needs to look for any, would be the design and synthesis new organic linkers involving multiple steps. Multistep organic synthesis generally results in small yields, which would prohibit the exploration and utilization of the exotic organic ligands. Though only a small hurdle, application potential of the MOFs is so high that it is highly likely that such of approaches would be pursued. The real issue and concern in this area would be the scaling-up of the laboratory synthesis procedure into economically at the viable industrial one. One can only be optimistic since it is at the early stages of development of this area.

## Acknowledgments

The authors are thankful for the Department of Science & Technology (DST), Government of India, for the award of research grants as well as for the INSPIRE faculty award (PM) and

the JC Bose Fellowship (SN). PM also thanks S.N. Bose National Centre for Basic Sciences, Kolkata and Director, Prof. A. K. Raychaudhuri for support and encouragement.

Received 3 November 2013.

## References

1. Special Issue on MOF, *Chem. Rev.* **2012**, *112*, 673–1268.
2. Special Issue on MOF, *Chem. Soc. Rev.* **2009**, *38*, 1213–1504.
3. Special Issue on MOF, *Eur. J. Inorg. Chem.* **2010**, 3683–3874.
4. S. M. Manocha, *Sadhana* **2003**, *28*, 335.
5. G. Ferey, *Chem. Soc. Rev.* **2008**, *37*, 191.
6. P. Mahata, S. Natarajan, *Chem. Soc. Rev.* **2009**, *38*, 2304.
7. F. A. A. Paz, J. Klinowski, S. M. F. Vilela, J. P. C. Tome, J. A. S. Cavaleiro, J. Rocha, *Chem. Soc. Rev.* **2012**, *41*, 1088.
8. T. R. Cook, Y. R. Zheng, P. J. Stang, *Chem. Rev.* **2013**, *113*, 734.
9. W. Xuan, C. Zhu, Y. Liu, Y. Cui, *Chem. Soc. Rev.* **2012**, *41*, 1677.
10. A. Phan, C. J. Doonan, F. J. Uribe-Romo, C. B. Knobler, M. O'Keeffe, O. M. Yaghi, *Acc. Chem. Res.* **2010**, *43*, 58.
11. S. Kitagawa, R. Kitaura, S. I. Noro, *Angew. Chem. Int. Ed.* **2004**, *43*, 2343.
12. P. Mahata, S. Natarajan, P. Panissod, M. Drillon, *J. Am. Chem. Soc.* **2009**, *131*, 10140.
13. P. Mahata, R. Raghunathan, D. Banerjee, D. Sen, S. Ramasesha, S. V. Bhat, S. Natarajan, *Chem. Asian J.* **2009**, *4*, 936.
14. P. Jain, N. S. Dalal, B. H. Toby, H. W. Kroto, A. K. Cheetham, *J. Am. Chem. Soc.* **2008**, *130*, 10450.
15. P. Mahata, S. Natarajan, *CrystEngComm.* **2009**, *11*, 560.
16. R. M. Barrer, *Hydrothermal Chemistry of Zeolites*, Academic Press, London, **1982**.
17. P. M. Foster, A. R. Burbank, C. Livage, G. Ferey, A. K. Cheetham, *Chem. Commun.* **2004**, 368
18. P. Mahata, M. Prabu, S. Natarajan, *Inorg. Chem.* **2008**, *47*, 8451
19. P. Mahata, A. Sundaresan, S. Natarajan, *Chem. Commun.* **2007**, 4471
20. P. M. Forster, P. M. Thomas, A. K. Cheetham, *Chem. Mater.* **2002**, *14*, 17.
21. D. Sarma, K. V. Ramanujachary, N. Stock and S. Natarajan, *Cryst. Growth Des.* **2011**, *11*, 1357.
22. H. Li, M. Eddaoudi, M. O'Keeffe, O. M. Yaghi, *Nature* **1999**, *402*, 276.
23. S. S. Y. Chui, S. M. F. Lo, J. P. H. Charmant, A. G. Orpen, I. D. Williams, *Science* **1999**, *283*, 1148.
24. D. Zacher, O. Shekhah, C. Wöll, R. A. Fischer, *Chem. Soc. Rev.* **2009**, *38*, 1418.
25. Z. Zhao, X. Ma, A. Kasik, Z. Li, Y. S. Lin, *Ind. Eng. Chem. Res.* **2013**, *52*, 1102.
26. J. Nan, X. Dong, W. Wang, W. Jin, N. Xu, *Langmuir* **2011**, *27*, 4309.
27. C. Serre, F. Millange, C. Thouvenot, M. Nogues, G. Marsolier, D. Louer, G. Ferey, *J. Am. Chem. Soc.* **2002**, *124*, 13519.
28. F. Millange, C. Serre, G. Ferey, *Chem. Commun.* **2002**, 822.



29. F. Millange, N. Guillou, R. I. Walton, J. M. Greneche, I. Margiolaki, G. Ferey, *Chem. Commun.* **2008**, 4732.
30. L. Alaerts, M. Maes, L. Giebeler, P. A. Jacobs, J. A. Martens, J. F. M. Denayer, C. E. A. Kirschhock, D. E. De Vos, *J. Am. Chem. Soc.* **2008**, *130*, 14170.
31. G. Ferey, C. Mellot-Draznieks, C. Serre, F. Millange, J. Dutour, S. Surble, I. Margiolaki, *Science* **2005**, *309*, 2040.
32. O. Ohmori, M. Kawano, M. Fujita, *Angew. Chem. Int. Ed.* **2005**, *44*, 1962.
33. T. Kawamichi, T. Haneda, M. Kawano, M. Fujita, *Nature* **2009**, *461*, 633.
34. Y. Inokuma, S. Yoshioka, J. Ariyoshi, T. Arai, Y. Hitora, K. Takada, S. Matsunaga, K. Rissanen, M. Fujita, *Nature* **2013**, *495*, 461.
35. Y. Q. Tian, C. X. Cai, J. Ji, X. Z. You, S. M. Peng, S. H. Lee, *Angew. Chem. Int. Ed.* **2002**, *41*, 1384.
36. Y. Q. Tian, C. X. Cai, X. M. Ren, C. Y. Duan, Y. Xu, S. Gao, X. Z. You, *Chem. Eur. J.* **2003**, *9*, 5673.
37. Y. Q. Tian, Z. X. Chen, L. H. Weng, H. B. Guo, S. Gao, D. Y. Zhao, *Inorg. Chem.* **2004**, *43*, 4631.
38. X. C. Huang, Y. Y. Lin, J. P. Zhang, *Angew. Chem. Int. Ed.* **2006**, *45*, 1557.
39. K. S. Park, Z. Ni, A. P. Cote, J. Y. Choi, R. Hunag, F. J. Uribe-Romo, H. K. Chae, M. O'Keeffe, O. M. Yaghi, *Proc. Natl. Acad. Sci. USA.* **2006**, *103*, 10186.
40. H. Hayashi, A. P. Cote, H. Furukawa, M. O'Keeffe, O. M. Yaghi, *Nat. Mater.* **2007**, *6*, 501.
41. R. Banerjee, A. Phan, B. Wang, C. Knobler, H. Furukawa, M. O'Keeffe, O. M. Yaghi, *Science* **2008**, *319*, 939.
42. T. Wu, X. Bu, R. Liu, Z. Lin, J. Zhang, P. Feng, *Chem Eur J.* **2008**, *14*, 7771.
43. B. Wang, A. P. Cote, H. Furukawa, M. O'Keeffe, O. M. Yaghi, *Nature* **2008**, *453*, 207.
44. R. Vaidhyanathan, D. Bradshaw, J.-N. Rebilly, J. P. Barrio, J. A. Gould, N. G. Berry, M. J. Rosseinsky, *Angew. Chem. Int. Ed.* **2006**, *45*, 6495.
45. S. C. Sahoo, T. Kundu, R. Banerjee, *J. Am. Chem. Soc.* **2011**, *133*, 17950.
46. T. Kundu, S. C. Sahoo, R. Banerjee, *Chem. Commun.* **2013**, *49*, 5262.
47. T. Kundu, S. C. Sahoo, R. Banerjee, *Cryst. Growth Des.* **2012**, *12*, 2572.
48. T. Kundu, S. C. Sahoo, R. Banerjee, *Cryst. Growth Des.* **2012**, *12*, 4633.
49. T. Kundu, S. C. Sahoo, R. Banerjee, *CrystEngComm.* **2013**, *15*, 9634.
50. D. Sarma, K. V. Ramanujachary, S. E. Lofland, T. Magdaleno, S. Natarajan, *Inorg. Chem.* **2009**, *48*, 11660.
51. R. A. Smaldone, R. S. Forgan, H. Furukawa, J. J. Gassenmith, A. M. Z. Slawin, O. M. Yaghi, J. F. Stoddart, *Angew. Chem. Int. Ed.* **2010**, *49*, 8630.
52. R. S. Forgan, R. A. Smaldone, J. J. Gassenmith, H. Furukawa, D. B. Cordes, Q. Li, C. E. Wilmer, Y. Y. Botros, R. Q. Snurr, A. M. Z. Slawin and J. F. Stoddart, *J. Am. Chem. Soc.* **2012**, *134*, 406.



**Partha Mahata** received his Ph.D. from Solid State and Structural Chemistry unit, Indian Institute of Science, Bangalore, India, in 2009. He joined as an Assistant Professor at Thapar University, Patiala, India in 2012 after his post-doctoral research in Tokyo University, Japan (2009–2011). Currently he is a faculty at department of Condensed Matter Physics and Material Sciences, S. N. Bose National Centre for Basic Sciences, Kolkata, India. His research interests include metal-organic materials for application in sensors, catalysis, storage and transports.



**Srinivasan Natarajan** presently a Professor at the Solid State and Structural Chemistry Unit, Indian Institute of Science. He has been a co-author of about 300 journal articles and book chapters. He is an elected Fellow of all the three Science Academies in India, and a JC Bose National Fellow. His research interests are in the area of solid state and materials chemistry, especially functional open-framework solids, inorganic pigments, Li-ion conductors for battery applications.

